Acta Crystallographica Section D
Biological Crystallography
ISSN 0907-4449

Crystal structure of equine apolactoferrin at 303 K providing further evidence of closed conformations of N and C lobes

Pravindra Kumar, Javed A. Khan, Savita Yadav and Tej P. Singh*

Department of Biophysics, All India Institute of Medical Sciences, New Delhi 110 029, India

Correspondence e-mail: tps@aiims.aiims.ac.in

Received 20 June 2001
Accepted 19 November 2001

PDB Reference: equine apolactoferrin, 1i6b.

Lactoferrin is an iron-binding protein. In the iron-bound state, the two domains of each lobe are invariably closed over an Fe^{3+} ion. On the other hand, the structures of iron-free forms of lactoferrins from various species show different domain orientations. In order to determine the effects of external conditions such as pH, temperature and the presence of other additive agents on the crystal packing and consequently the influence of crystal packing forces on the final conformations of the two lobes of apolactoferrin, the structure of equine apolactoferrin has been determined at 303 K. The equine apolactoferrin was crystallized at 303 K using a microdialysis setup in which the concentration of protein was kept at 70 mg ml^{-1} in 0.025 *M* Tris–HCl pH 8.0 with a reservoir containing 19% ethanol in the same buffer. The structure has been determined by molecular replacement using equine diferric lactoferrin as a model and was refined to an *R* factor of 0.23. The value of the overall *B* factor in the present structure is 81.3 Å^2. The overall structure of the protein is similar to its earlier structure based on crystals grown at 277 K as well as that of diferric equine lactoferrin. The N and C lobes have been found to be slightly differently oriented (4.9 and 7.1°, respectively) compared with the structures of equine diferric lactoferrin and apolactoferrin analyzed at 277 K, but the domain orientations in the two structures are identical as they remain closed over the empty iron-binding cleft. Overall, the structures of equine diferric lactoferrin, equine apolactoferrin at 277 K and the present structure of equine apolactoferrin at 303 K display identical domain orientations, suggesting that variation in the temperature of crystal growth, data collection and the processes of iron binding and iron release do not influence the arrangements of domains in equine lactoferrin.

1. Introduction

Lactoferrin, an iron-binding 80 kDa glycoprotein, is a member of the transferrin family. It consists of two homologous N and C lobes which are made up of two domains N1 and N2, and C1 and C2, respectively. The crystal structures of fully iron-saturated diferric forms of lactoferrin (Anderson *et al.*, 1989; Moore *et al.*, 1997; Sharma, Paramasivam *et al.*, 1999; Kumar *et al.*, 2001; Karthikeyan *et al.*, 1999, 2000) have revealed that the two domains of each lobe are closed in an identical manner over an Fe^{3+} ion. Four of the six Fe^{3+} coordination sites in the closed lactoferrin structure are occupied by protein ligands (two Tyr residues, one Asp and one His) and the other two by a bidentate carbonate ion.

On the other hand, structures of iron-free forms of lactoferrin have shown large-scale structural variations (Jameson *et*

al., 1998; Sharma, Rajshankar *et al.* 1999; Khan, Kumar, Paramasivam *et al.*, 2001). For example, the structure of an iron-free form of equine lactoferrin (EALF4; Sharma, Rajshankar *et al.*, 1999) indicated closed conformations for both lobes, which were indistinguishable from those of diferric equine lactoferrin (ELF; Sharma, Paramasivam *et al.*, 1999). The human apolactoferrin structure (HALF; Jameson *et al.*, 1998) showed an opened N lobe and a closed C lobe, while in camel apolactoferrin (UALF; Khan, Kumar, Paramasivam *et al.*, 2001) both lobes adopted open conformations. It may be mentioned here that studies using X-ray scattering techniques have indicated open conformations for both lobes in human apolactoferrin in solution (Grossman *et al.*, 1992). In view of the above observations, it has been a matter of intense debate (Anderson *et al.*, 1990; Sharma, Rajshankar *et al.*, 1999; Baker *et al.*, 1999; Khan, Kumar, Paramasivam *et al.*, 2001) whether the variations in conformations of apolactoferrins as indicated by crystal structures were species specific or whether it was a matter of random selection by crystalline state from a pool of closed and opened conformations which exist in equilibrium in solution. In order to establish the basis of these variations and their possible relationships to species-specific functions, it is necessary to determine the crystal structures of various apoproteins under different solvent, temperature and pH conditions. Here, we report the crystal structure of equine apolactoferrin (EALF30) at 3.2 Å resolution based on the data obtained at 303 K from crystals grown at 303 K. The previously reported structure of equine apolactoferrin at 3.8 Å resolution was based on crystals grown at 277 K from which intensity data were collected using a synchrotron beamline (EALF4; Sharma, Rajshankar *et al.*, 1999). The structures of various cation- and anion-substituted equine lactoferrins have also been determined using crystals grown at 277 K (Sharma, Paramsivam *et al.*, 1999; Sharma & Singh, 1999*a*,*b*; Kumar *et al.*, 2000, 2001; Sharma *et al.*, 2001).

2. Experimental

2.1. Stepwise iron removal from lactoferrin

The protein was purified from fresh samples of equine colostrum. The purified samples of equine lactoferrin were saturated with iron following the procedure of Mazurier & Spik (1980). The iron content was estimated using the procedure of Wootton (1964). The purified iron-saturated lactoferrin (1%) in 50 m*M* Tris–HCl buffer at pH 8.0 was dialyzed against an excess of 0.1 *M* citrate buffer with regular changes after every 6 h at 277 K. The dialysis was carried out at different values of pH for 24 h in each case, starting from pH 8.0 and ending at pH 2.0 with pH intervals of 0.5. At every pH, iron saturation was estimated from the ratio A_{465}/A_{280}. Similar steps were followed for camel and buffalo lactoferrins.

2.2. Stepwise iron saturation of lactoferrin

The iron-saturated lactoferrin was prepared following the procedure of Mazurier & Spik (1980). Purified apolactoferrin was dissolved in 1 ml of 0.1 *M* citrate buffer to a final concentration of 100 mg ml^{-1}. $FeCl_3.6H_2O$ was added to give an iron saturation of ~110%. The protein was then dialyzed against citrate buffer pH range 2.0–8.0 with pH increments of 0.5 at 277 K. At every pH dialysis was carried out for 24 h with regular changes of reservoir buffer at every 6 h. The iron saturation was estimated at every pH using the ratio A_{465}/A_{280}.

2.3. Crystallization at 303 K

The purified equine apolactoferrin obtained from fresh colostrum samples was used for crystallization. In the previous study (Sharma, Rakshankar *et al.*, 1999), it was crystallized at 277 K by microdialysis with a protein concentration of 40 mg ml^{-1} in 0.01 *M* Tris–HCl using 10%(*v*/*v*) ethanol in the same buffer at pH 8.5. All the values mentioned here were estimated at 277 K. In the present study, the crystals of equine apolactoferrin were obtained at 303 K using microdialysis. The protein concentration was kept at 70 mg ml^{-1} in 0.025 *M* Tris–HCl pH 8.0. It was dialyzed against the same buffer containing 19%(*v*/*v*) ethanol. All the crystallization setups were placed in a constant-temperature room maintained at 303 K. All the values including pH in the present experiment were determined at 303 K. The irregular-shaped colourless crystals grew in three weeks to dimensions of 0.5 × 0.3 × 0.3 mm.

2.4. Data collection and processing

The X-ray intensity data to 3.2 Å resolution were collected at 303 K using a 300 mm MAR Research imaging-plate scanner and Cu $K\alpha$ radiation generated from an RU-200 rotating-anode X-ray generator (Rigaku) operating at 40 kV and 100 mA. The room temperature during data collection was maintained at 303 K with the help of a local air-conditioning system. Although crystals diffracted to 3.0 Å, the completeness beyond 3.2 Å was lower than 20%. Therefore, the final data set was obtained to 3.2 Å resolution. The data were processed using the *HKL* package (Otwinowski & Minor, 1997). The crystals belong to the orthorhombic space group $P2_12_12_1$ with one molecule in the asymmetric unit. The unit-cell parameters are a = 80.4, b = 103.4, c = 112.1 Å. Assuming one molecule of the protein in the asymmetric unit and a molecular weight of 80 kDa, the V_M value was calculated to be 2.92 Å^3 Da^{-1}. The unit-cell parameters and hence V_M of the present structure are significantly different from those reported earlier for crystals grown at 277 K. This effect might have been caused by a loosening of the molecules in crystals owing to the elevated external temperature. The details of the crystallographic data and their comparison with values reported earlier at 277 K as well as those of diferric equine lactoferrin are given in Table 1.

2.5. Structure determination and refinement

So far, structures of three apolactoferrins from three different sources, namely equine, human and camel, have been determined. These were found in different conformational states such as closed–closed, open–closed and open–open, thus making them uncertain models for molecular-replace-

Table 1
Summary of data-collection statistics and comparision of crystallographic data for EALF30, EALF4 and ELF.

Values in parentheses are for the outer resolution shell.

	EALF30	EALF4	ELF
Crystallization temperature (K)	30	4	4
Precipitating agent	Ethanol	Ethanol	Ethanol
Concentration of precipitating agent (%)	19	10	10
pH of buffer	8.0	8.5	8.5
Space group	$P2_12_12_1$	$P2_12_12_1$	$P2_12_12_1$
Unit-cell parameters (Å)			
a	80.4	77.4	85.2
b	103.4	100.4	99.5
c	112.1	102.6	103.1
Matthews coefficient (V_M) (Å^3 Da^{-1})	2.92	2.49	2.72
Solvent content (%)	58	51	55
Resolution range (Å)	20.0–3.2	20.0–3.8	20.0–2.6
Total No. of reflections	67331	101096	100182
No. of unique reflections	15800	7887	25558
R_{sym} (%)	11.0 (38.0)	12.0 (28.0)	6.3 (14.2)
$I/\sigma(I)$	9.6 (2.6)	6.5 (3.2)	12.5 (6.3)
Overall completeness (%)	99.4 (94.7)	99.1 (60.0)	99.8 (80.5)

ment calculations for each other. In the present case, owing to different conditions of crystal growth, the resulting conformation of the protein could not be predicted. Therefore, the structure determination had to be pursued by the molecular-replacement method (Rossmann, 1972; Navaza, 1994) using various models of holo and apolactoferrins. It may be noted that the available structures of ELF and EALF4 were identical. The structure of EALF4 was determined at 3.8 Å resolution, while that of ELF was carried out at 2.6 Å. Since the ELF structure was more accurate than EALF4, it was used as a model for the structure determination of EALF30. It gave a clear solution with a correlation coefficient of 64%. The model obtained from molecular replacement was refined using the program *X-PLOR* (Brünger *et al.*, 1987; Brünger, 1992*a*). A randomly chosen 5% of the reflections in the data set were used for R_{free} calculations (Brünger, 1992*b*). Rigid-body refinement, taking the N lobe (residues 1–344) and the C lobe (residues 345–689) as two separate rigid bodies, lowered the *R* factor to 0.381 (R_{free} = 0.44). Further cycles of refinement and model building using positional and prepstage in the *X-PLOR* protocol lowered the *R* factor to 0.31 (R_{free} = 0.40). The $2F_o - F_c$ and $F_o - F_c$ electron-density maps of the iron-binding clefts were critically examined to detect any density for the metal ions. However, no such density was detected even at as low a cutoff as 0.3σ in these maps, suggesting that the Fe^{3+} ions were absent in this structure. Subsequent refinement cycles of simulated annealing (Brünger *et al.*, 1990) and restrained least-squares refinement followed by manual model building (Jones *et al.*, 1991) were carried out to improve the model. Further energy minimization by a number of steps of positional (*xyz*) refinement followed by several steps of group *B*-factor refinement (two *B*-factor groups for each residue; one for backbone and one for side-chain atoms) led to a drop in the *R* factor to 0.23 for all data and a fall in R_{free} to 0.29.

3. Results and discussion

3.1. pH-induced release of iron from lactoferrins

Lactoferrin has two independent metal-binding sites per molecule of protein. The results of our comparative study of the desaturation of equine lactoferrin, buffalo lactoferrin and camel lactoferrin carried out under identical conditions are shown in Fig. 1. Similar data on human lactoferrin were also available in the literature (Mazurier & Spik, 1980). As seen from Fig. 1, the release of iron from equine and buffalo lactoferrins follows a single-step process. The onset of iron release in buffalo lactoferrin occurs at a pH > 5.5, while in equine lactoferrin it begins only at pH 4.0. On the other hand, the removal of iron from camel lactoferrin is clearly a two-step process in which 50% of the iron is lost at pH > 6.5, while the remaining 50% is released only at a pH less than 4.0. These data indicate that the release of iron from equine lactoferrin begins at a lower pH than observed in other lactoferrins and that both the clefts seem to function in a similar way.

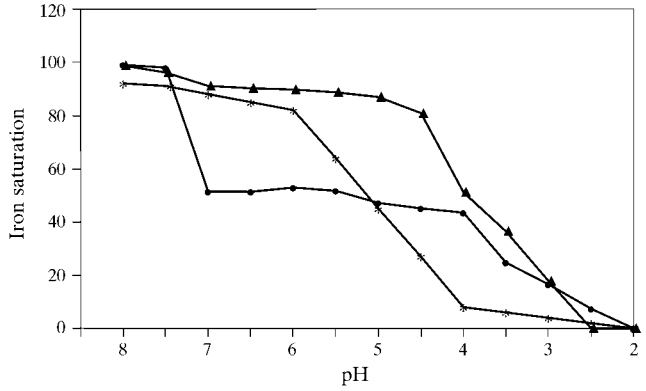

Figure 1
Effect of progressive reduction of pH on the removal of iron from lactoferrin. The curves represent the patterns for equine (triangles), buffalo (asterisks) and camel (circles) lactoferrins.

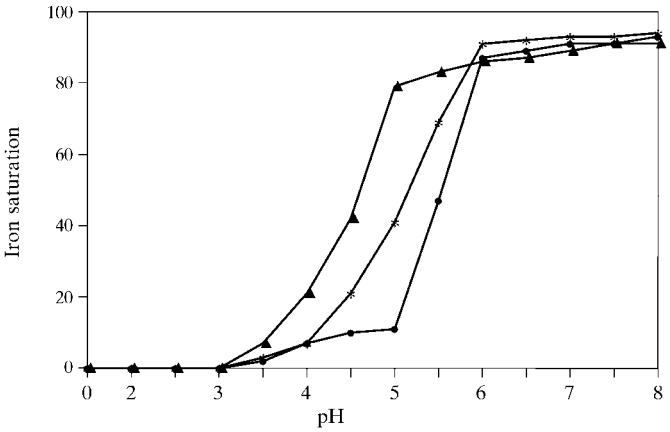

Figure 2
Comparative study of the iron saturation of equine lactoferrin. The curves represent the patterns for equine lactoferrin (triangles), buffalo lactoferrin (asterisks) and camel lactoferrin (circles).

3.2. pH-induced iron-binding in lactoferrin

The results of the comparative study of the iron saturation of equine, buffalo and camel lactoferrins are shown in Fig. 2. The process of iron absorption in equine lactoferrin begins early and it becomes fully saturated at pH < 5.0. It may be noted that in the other two examples of buffalo and camel lactoferrins the onset of iron binding begins at a similar pH value, but the complete saturation with iron occurs at a pH higher than 5.5. The reported results on iron saturation of human lactoferrin also indicated that the complete iron saturation was achieved at pH > 5.5 (Mazurier & Spik, 1980). Thus, it can be stated that the complete iron saturation in equine lactoferrin is achieved at a pH lower than that observed in buffalo, camel and human lactoferrins.

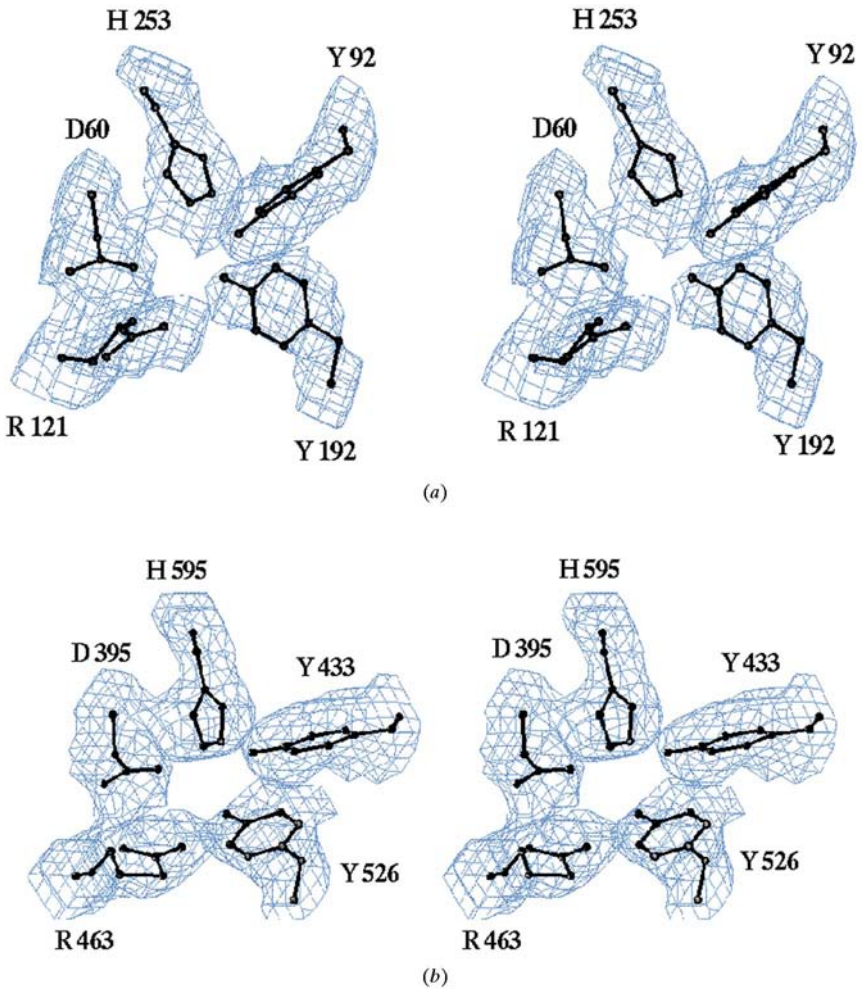

Figure 3
(*a*) Stereoview of the final ($2F_o - F_c$) electron-density map at the iron-binding site for the N lobe. The map is contoured at 0.3σ. The iron site is empty. (*b*) Stereoview of the final ($2F_o - F_c$) electron-density map at the iron-binding site for the C lobe. The map is contoured at 0.3σ. The iron site is empty.

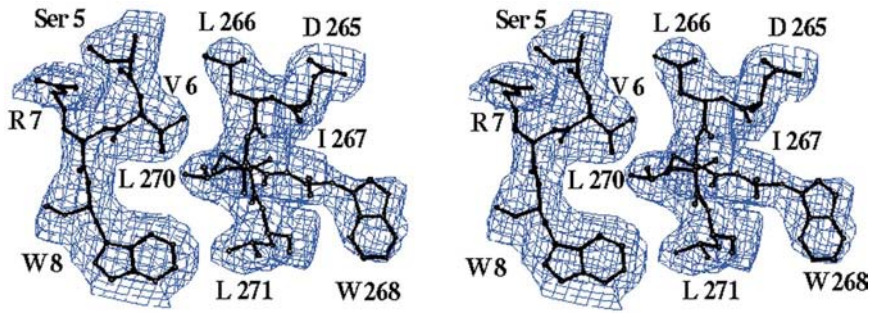

Figure 4
Stereoview of the electron-density map ($2F_o - F_c$) at 1.5σ for a representative region. Residue numbers are indicated.

3.3. Final model

The final coordinate set contains 5281 protein atoms from 689 amino-acid residues. As seen from the final $2F_o - F_c$ electron-density maps of the iron-binding clefts of the N and C lobes, the Fe^{3+} ions are absent in this structure, whereas the iron-binding ligands are well defined (Fig. 3). The observed overall mean *B* factor of 81.3 Å^2 is rather high. It is presumably a consequence of the elevated temperature of 303 K at which the crystals were grown and at which the data were collected. The *B* value calculated from a Wilson plot (Wilson, 1942) was found to be 85.6 Å^2. A considerable number of side chains on the surface of the molecule, particularly four residues at the N-terminus, the 84–87 loop in the N1 domain and the loop 418–424 in the C1 domain, had weak electron densities and very high *B* factors (∼103 Å^2). The rest of the structure is well defined, however, and in the final $2F_o - F_c$ electron-density map there are no breaks in the main-chain density when contoured at the 1σ level. It may be mentioned here that the overall mean *B* factor for diferric bovine lactoferrin was also considerably high at 71.4 Å^2 (Moore *et al.*, 1997). It may also be noted that the crystals of bovine lactoferrin were grown at 277 K and the X-ray intensity data were collected at room temperature (Moore *et al.*, 1997). The present protein structure has a geometry close to ideal, with r.m.s. deviations of 0.011 Å and 1.7° from standard values of bond lengths and angles, respectively. The final *R* factor was 0.23 for all reflections to 3.2 Å resolution. A section of representative electron density from a final ($2F_o - F_c$) map is shown in Fig. 4. A Ramachandran plot of the main-chain torsion angles (φ, ψ) (Ramachandran & Sasisekaran, 1968) shows that 80.1% of the

residues were in the most favoured regions as defined in the program *PROCHECK* (Laskowski *et al.*, 1993). Only two residues, Leu299 and Leu640, were present in the disallowed regions. These are parts of two γ-turns (Matthews, 1972) with torsion angles around 70, -60° (Baker & Hubbard, 1984). These two γ-turns are conserved in the N and C lobes of lactoferrin, transferrin and ovotransferrin structures, where they form part of one wall of each binding cleft.

3.4. Overall molecular structure

The overall molecular structure of EALF30 is shown in Fig. 5. The protein is folded into two lobes designated as the N and C lobes, each of which is divided into two domains N1 and N2, and C1 and C2, respectively. The high level of sequence identity (38.9%) between the two halves of the molecule is reflected in a very similar folding of the polypeptide chain in the two lobes. The superposition of C^α positions of the N and C lobes shows an r.m.s. difference of 1.06 Å. In order to obtain the best fit of the two lobes, first the C1 domain was superimposed on the N1 domain and then the C2 domain was rotated by 1.7° to match the N2 domain. The small value of the domain rotation indicates that the domain orientations in the two lobes are essentially similar. The corresponding angles in EALF4 and ELF were also found to be small, with values of 1.7 and 1.2°, respectively. This clearly showed that the overall structures of the two lobes and the orientations of the domains in the N and C lobes of EALF30, EALF4 and ELF were identical.

3.5. Structure comparison

The structure of EALF30 was compared by superimposing it on the previously determined structures of EALF4 and ELF using *LSQMAN* by minimizing the r.m.s. deviations of the main-chain atoms. When the N lobe of EALF30 was superimposed on the N lobe of EALF4, an additional rotation angle of 7.1° was required for the best fit of the C lobes of the two structures. The corresponding angle after superimposing the structures of EALF30 and ELF in a similar fashion was found to be 4.9°. These values indicate that the lobe orientations in EALF30, EALF4 and ELF were only slightly different. The r.m.s. deviations for C^α atoms of the complete molecules of EALF30 and EALF4 and of EALF30 and ELF were found to be 1.03 and 0.87 Å, respectively. The four protein ligands Asp60 (395), Tyr92 (433), Tyr192 (526) and His253 (595) in EALF30 and ELF showed some variations in their orientations, indicating that these residues were relatively flexible in the absence of a ferric ion. Further examination of interdomain interactions in EALF30, EALF4 and ELF indicated the presence of similar contacts in all three structures.

3.6. Domain arrangement

In the present high-temperature structure, both lobes adopt closed conformations with domain orientations identical to that observed in the 277 K structure of equine apolactoferrin (Sharma, Rajshankar *et al.*, 1999) and diferric equine lactoferrin (Sharma, Paramasivam *et al.*, 1999). This consistency in the arrangements of domains in various states of equine lactoferrin indicates a clear preference for adopting closed–closed conformations for its empty lobes. This indeed is in striking contrast to the open–closed and open–open conformations observed for human and camel lactoferrins, respectively. The closure and opening of the empty lobes is apparently dependent on the combined effect of interdomain interactions and the flexibility of the hinge region. The hinge regions in lactoferrins involve two antiparallel strands, *e* (Thr90–Val98) and *j* (Cys245–Ala254) in the N lobe, and the corresponding *e* (Gly432–Lys441) and *j* (Leu589–Val598) in the C lobe which run behind the iron-binding site connecting the N1 and N2, and the C1 and C2 domains. So far, the detailed structures of three apolactoferrins from human, horse and camel are known. Unfortunately, the structure of the iron-saturated form of camel lactoferrin is not yet known. Therefore, a detailed comparison between the iron-saturated and iron-free structures of camel lactoferrin is not possible. In view of this, a comparison of interdomain interactions and the flexibility of the *e* and *j* strands can be made only in human and equine lactoferrins. The sequence comparisons of the *e* and *j* strands in the equine and human lactoferrins are shown in Fig. 6. Despite high sequence identities in these regions, there are critical residues that seem to be responsible for the observed variations in the flexibilities of these strands in the equine and human lactoferrins. For example, in the *e* strand of ELF, residue 91 is Arg, while the corresponding residue in HLF is His. Arg91 in ELF forms two hydrogen bonds with the backbone O atom of Leu687. The residue 687 is part of the C-terminal helix. The corresponding His91 in HLF is not involved in a similar interaction with other parts of the protein. In the identical sequences of the *j* strands of ELF and HLF, the only interesting residue is Arg249. In ELF it interacts with Glu89 $O^{\varepsilon 1}$ and forms two hydrogen bonds (Fig. 7). The corresponding Arg249 in HLF faces Arg89, thus promoting repulsion. Clearly, the *e* and *j* strands in ELF are held by attractive interactions with other parts of the protein, thus imparting a moderate rigidity to them. The corresponding interactions in HLF are either absent or repulsive in nature, thus enhancing the flexibility of these strands in the N lobe. Summing up, it is clearly observed that the *e* and *j* strands in equine lactoferrin are apparently held through various attractive interactions, while in human lactoferrin these interactions are either weak or absent, thus making the hinge region flexible.

3.7. Crystal packing

The overall arrangements of molecules in the crystals of EALF30, EALF4 and ELF were similar, although in the crystals of EALF30 considerable effects of higher temperature were observed in which the unit-cell parameters were in general found to be significantly larger than those observed in EALF4 and ELF (Table 1). The difference in the length of the *c* axis was the most pronounced. As a result of the expansion of unit-cell volume, the solvent content in EALF30 was calculated to be more than that of EALF4 and ELF, indicating

a relatively loose packing of the molecules in EALF30. Since ELF and EALF4 were reported to be identical and as the structure of ELF was more accurate, a subsequent comparison of molecular packing was carried out between EALF30 and ELF. As seen from Figs. 8(*a*) and 8(*b*), the original molecule *A* has been drawn together with its four nearest symmetry-related molecules *B*, *C*, *D* and *E* for EALF30 and ELF, respectively. The interactions of molecule *A* with molecules *B*, *C*, *D* and *E* have been examined in both EALF30 and ELF. Glu343 $O^{\varepsilon 2}$ of molecule *A* interacts with Ser480 O^{γ} of molecule *B* in ELF. The corresponding pair of atoms in EALF30 are 9.6 Å apart, showing no interaction. In ELF, Asn421 $N^{\delta 2}$ and Asn621 O of molecule *A* form strong hydrogen bonds with Arg30 O and Trp268 $N^{\varepsilon 1}$, respectively, of the symmetry-related molecule *B*. The corresponding distances between the pairs of same molecules in EALF30 are 6.6 and 8.6 Å, respectively. In contrast, Gly620 O and Pro623 O of molecule *A* form hydrogen bonds with Arg273 $N^{\eta 2}$ and His272 $N^{\varepsilon 2}$ of molecule *B* in EALF30, while the corresponding distances in ELF are 5.8 and 6.7 Å, respectively. However, Ser102 O and Gly202 O of molecule *A* participate in hydrogen-bond formation with Gly653 N and Glu605 $N^{\varepsilon 2}$ of molecule *C* in both the EALF30 and the ELF structures, showing identical interactions. The molecule *D* does not interact directly with molecule *A*, although it makes some interactions through solvent molecules. Furthermore, there are two regions of molecules *A* and *E* that are involved in extensive interactions with each other. Of a total of eight possible hydrogen bonds, six are well formed in ELF, while seven good hydrogen bonds are observed in EALF30. These values are listed in Table 2. These observations indicate that minor differences do occur in the orientations of the equine lactoferrin molecules in the crystals which might have been caused solely by the conditions of crystallization and more significantly by the temperature at which crystallization was carried out. One of the most apparent effects of crystallization and data-collection conditions is seen in the form of the overall mean *B* factors of 81.3, 41.2 and 32.6 $Å^2$ for EALF30, EALF4 and ELF, respectively.

4. Conclusions

Although the present high-temperature structure lacks accuracy owing to poor crystal quality and high *B* factors, it does provide a basis for a generalization of the arrangements of domains in the iron-saturated and iron-free forms of equine

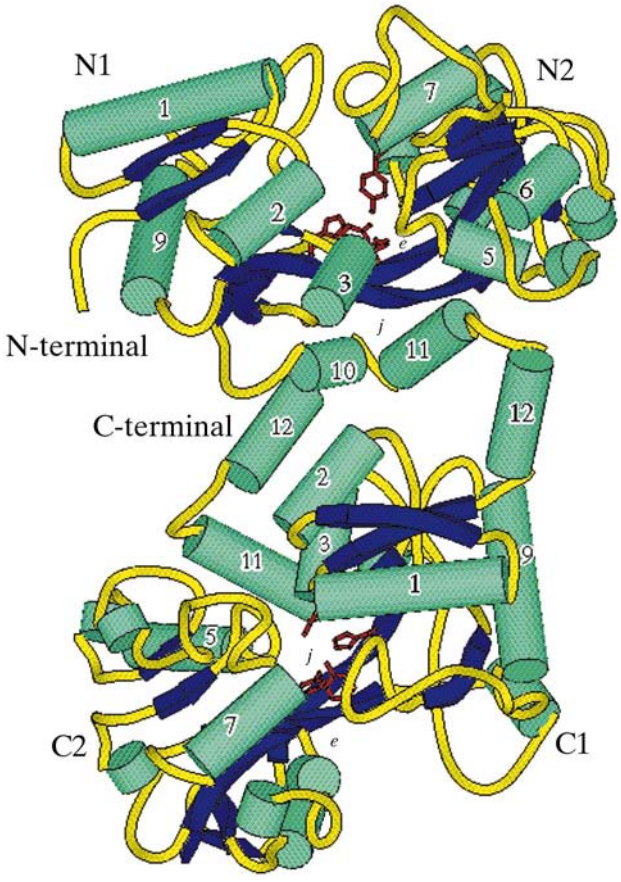

Figure 5
Schematic diagram of equine apolactoferrin showing the arrangement of the four domains in the proteins. The figure also shows the residues which are involved in iron binding in diferric lactoferrin. Selected α-helices and β-strands are numbered. The figure was drawn using *MOLSCRIPT* (Kraulis, 1991).

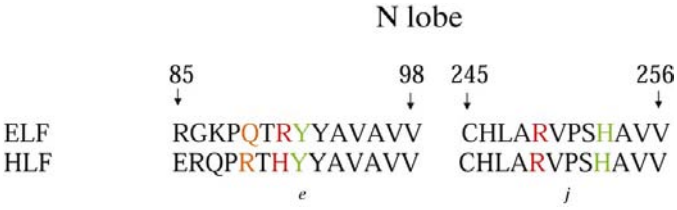

Figure 6
The sequence comparisons of selected segments of hinge regions consisting of *e* and *j* strands in equine (ELF) and human (HLF) lactoferrins. The residues involved in critical interactions are marked in red and those involved in iron binding are indicated in green. The numbering scheme used is that of equine lactoferrin.

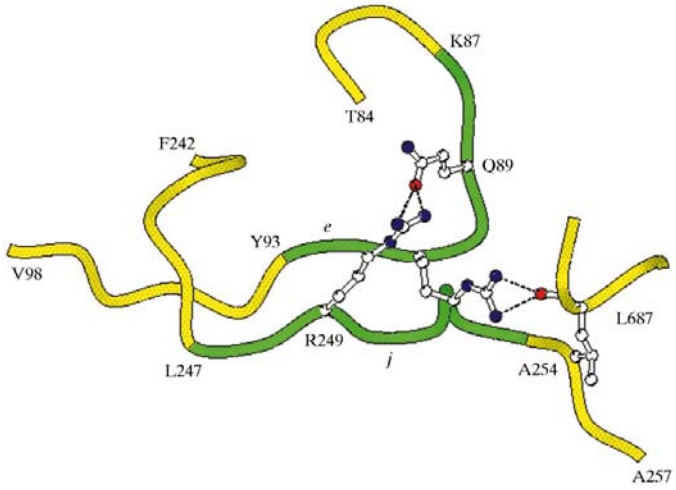

Figure 7
The critical interactions involving residues of the hinge regions in the N lobe of ELF. The hinge is indicated in green.

Table 2
Selected intermolecular distances (Å) in ELF and EALF30.

Domains (for residue 1)	Residue 1 (molecule *A*)	Residue 2 (symmetry-related molecules *B*/*C*/*D*/*E*)	Domains (for residue 2)	ELF	EALF30
C1	Glu343 $O^{\varepsilon 2}$	Ser480 O^{γ} (*B*)	C2	2.9	9.6
C1	Asn421 $N^{\delta 2}$	Arg30 O (*B*)	N1	2.8	6.6
C1	Asn621 O	Trp268 $N^{\varepsilon 1}$ (*B*)	N1	2.9	8.6
C1	Pro623 O	His272 $N^{\varepsilon 2}$ (*B*)	N1	5.8	3.2
C1	Gly620 O	Arg273 $N^{\eta 2}$ (*B*)	N1	6.7	3.2
N2	Ser102 O	Gly653 N (*C*)	C1	3.2	3.1
N2	Gly202 O	Gln605 $N^{\varepsilon 2}$ (*C*)	C1	3.2	3.2
N1	Arg3 $N^{\eta 1}$	Asp225 $O^{\delta 2}$ (*E*)	N2	3.0	3.1
N1	Arg3 $N^{\eta 1}$	Glu221 $O^{\varepsilon 2}$ (*E*)	N2	3.0	6.7
C2	Glu510 O	Lys21 N^{ζ} (*E*)	N1	3.1	3.2
C2	Glu510 $O^{\varepsilon 2}$	Arg24 $N^{\eta 1}$ (*E*)	N1	3.0	2.8
C2	Glu510 Oe2	Arg24 N^{ε} (*E*)	N1	5.1	3.0
C2	Glu510 O	Arg24 $N^{\eta 2}$ (*E*)	N1	3.0	2.9
C2	Glu512 $O^{\varepsilon 2}$	Lys21 N^{ζ} (*E*)	N1	3.0	3.1
C2	Glu512 $O^{\varepsilon 1}$	Lys21 N^{ζ} (*E*)	N1	5.4	3.1

lactoferrins. The crystals of EALF30 and EALF4 were grown at two significantly different temperatures. Similarly, the intensity data were also collected at different temperatures. In spite of distinctly different conditions of temperature, only small variations occurred in the crystal packings. The two molecular structures were found to be essentially similar. Furthermore, the orientations of domains in these structures did not alter, although the orientations of the lobes varied slightly. However, these conditions seemed to have contributed to a high value of the overall mean *B* factor of the present structure. It is of particular interest that the domains in both the N and C lobes of equine lactoferrin remain closed in all the conditions. This observation is clearly supported by iron-binding and iron-release experiments. The examination of interactions involving the *e* and *j* strands indicate a lower flexibility in the hinge regions of equine lactoferrin. Therefore, a strong preference for the closed-lobe conformations in equine lactoferrin can be expected. In view of this, it may be stated that the processes of iron-binding and iron-release and the mild crystal packing forces may not be able to perturb the domain orientations in equine lactoferrin. Unlike the closed conformations of N and C lobes in various states of equine apolactoferrin, the domain arrangements in human and camel apolactoferrins showed drastic yet different changes in domain orientations upon iron binding and iron release. In human apolactoferrin the N lobe adopted the open and the C lobe preferred the closed conformation (Jameson *et al.*, 1998). There are also reports of observing open conformations for both the N and C lobes in human apolactoferrin (Baker *et al.*, 1997). The analysis of interactions in the hinge region of human lactoferrin indicates that the C lobe is less flexible than the N lobe. This means that the N lobe may be influenced more readily by the process of iron binding and release. It could also mean that the equilibrium of closed and open states of the N and C lobes in human apolactoferrin can be shifted. On the other hand, in camel apolactoferrin both lobes were found in the open conformation in two different states (Khan, Kumar, Paramasivam *et al.*, 2001; Khan, Kumar, Srinivasan *et al.*, 2001). Further comparison is not possible in camel lactoferrin owing to unavailability of the iron-saturated closed–closed structure. In any case, the studies carried out so far indicate that the observed orientations of domains in the crystals of various apolactoferrins might have a species-related preferences. Finally, assuming that these domain arrange-

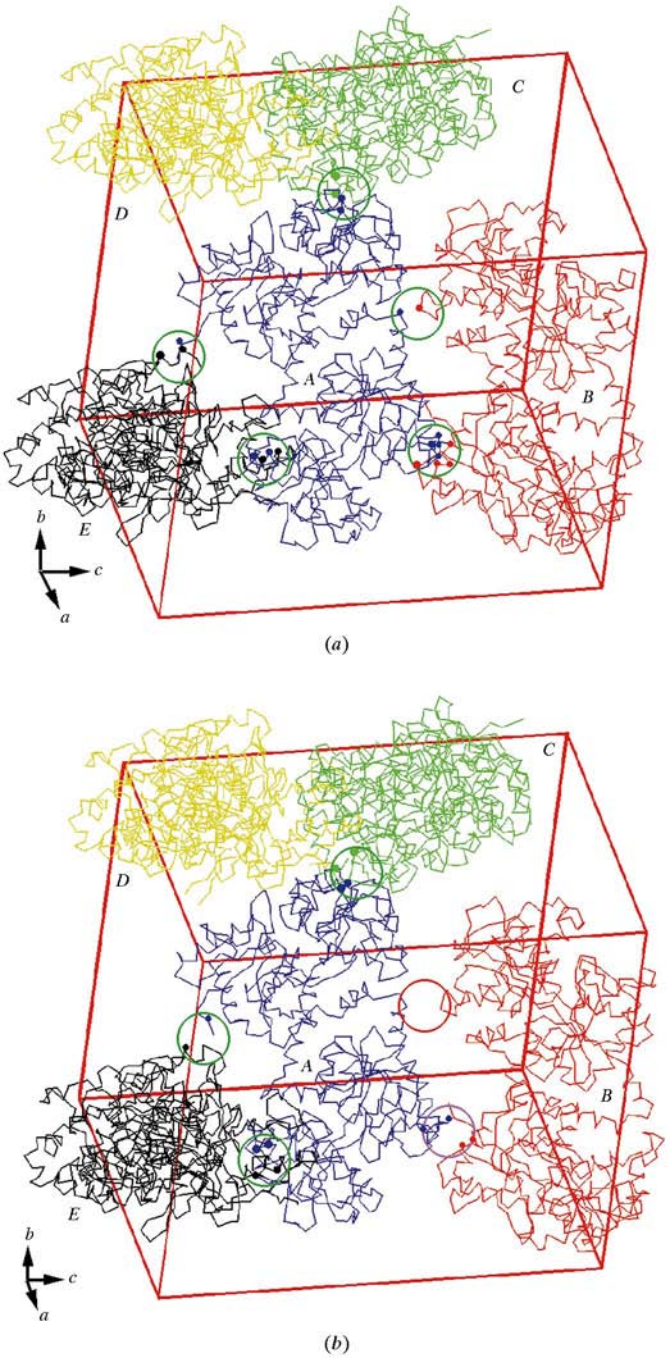

Figure 8
(*a*) Molecular packing in the crystals of EALF30. Molecule *A* is the original molecule. *B*, *C*, *D* and *E* are symmetry-related nearest neighbours. Circles indicate contact regions. Solid circles are the participating residues (Table 2). (*b*) Molecular packing in the crystals of ELF. Molecule *A* is the original molecule. *B*, *C*, *D* and *E* are symmetry-related nearest neighbours. Circles indicate contact regions. Solid circles are the participating residues (Table 2).

ments are species specific, the fundamental question still remains as to the functional implications of these observations. To gain further insight into these aspects, the structures of lactoferrins from various species under different conditions of crystallization and data collection are required in both iron-saturated and iron-free forms.

This work was supported by a grant from the Department of Biotechnology of the Ministry of Science and Technology, New Delhi. PK thanks the Council of Scientific and Industrial Research (CSIR), New Delhi for the award of a senior research fellowship.

References

Anderson, B. F., Baker, H. M., Norris, G. E., Rice, D. E. & Baker, E. N. (1989). *J. Mol. Biol.* **209**, 711–734.

Anderson, B. F., Baker, H. M., Norris, G. E., Rumball, S. V. & Baker, E. N. (1990). *Nature (London)*, 344, 784–787.

Baker, E. N., Anderson, B. F., Baker, H. M., Faber, H. R., Smith, C. A. & Sutherland-Smith, A. J. (1997). *Interactions and Biological Functions*, edited by T. W. Hutchens & B. Lonnerdal, pp. 177–191. Totowa, NJ, USA: Humana Press.

Baker, E. N. & Hubbard, R. E. (1984). *Prog. Biophys. Mol. Biol.* **44**, 97–179.

Baker, H. M., Anderson, B. F., Baker, E. N., Kidd, R. D., Shewry, S. C. & Baker, E. N. (1999). In *Lactoferrin: Structure, Function and Applications. Proceedings of the 4th International Conference on Lactoferrin*, edited by K. Shimazaki, H. Tsuda, M. Tomita, T. Kuwata & J. P. Perraudin. Amsterdam: Elsevier.

Brünger, A. T. (1992*a*). *X-PLOR v3.1 User's Guide. A System for X-ray Crystallography and NMR.* New Haven, Connecticut: Yale University Press.

Brünger, A. T. (1992*b*). *Nature (London)*, **355**, 472–474.

Brünger, A. T., Krukowski, A. & Erickson, J. (1990). *Acta Cryst.* A**46**, 585–593.

Brünger, A. T., Kuriyan, J. & Karplus, M. (1987). *Science*, **235**, 458–460.

Grossman, J. G., Neu, M., Pantos, E., Schab, F. J., Evans, R. W., Townes-Andrews, E., Lindley, P. F., Appel, H., Thies, W. G. & Hasnain, S. S. (1992). *J. Mol. Biol.* **225**, 811–819.

Jameson, G. B., Anderson, B. F., Norris, G. E., Thomas, H. D. & Baker E. N. (1998). *Acta Cryst.* D**54**, 1319–1335.

Jones, T. A., Zou, J., Cowan, S. & Kjeldgaard, W. J. M. (1991). *Acta Cryst.* A**47**, 110–119.

Karthikeyan, S., Yadav, S., Paramasivam, M., Srinivasan, A. & Singh, T. P. (1999). *Acta Cryst.* D**55**, 1805–1813.

Karthikeyan, S., Yadav, S., Paramasivam, M., Srinivasan, A. & Singh, T. P. (2000). *Acta Cryst.* D**56**, 684–689.

Khan, J. A., Kumar, P., Paramasivam, M., Yadav, R. S., Sahani, M. S., Sharma, S., Srinivasan, A. & Singh, T. P. (2001). *J. Mol. Biol.* **309**, 751–782.

Khan, J. A., Kumar, P., Srinivasan, A. & Singh, T. P. (2001). *J. Biol. Chem.* **276**, 36817–36823.

Kraulis, P. J. (1991). *J. Appl. Cryst.* **24**, 946–950.

Kumar, S., Sharma A. K., Paramasivam, M., Srinivasan, A. & Singh, T. P. (2001). *Ind. J. Biochem. Biophys.* **38**, 135–141.

Kumar, S., Sharma, A. K. & Singh, T. P. (2000). *Ind. J. Phys. B*, **74**, 103–108.

Laskowski, R. A., MacArthur, M. W., Moss, D. S. & Thornton, J. M. (1993). *J. Appl. Cryst.* **26**, 283–291.

Matthews, B. W. (1972). *Macromolecules*, **5**, 818–819.

Mazurier, J. & Spik, G. (1980). *Biochim. Biophys. Acta*, **629**, 399–408.

Moore, S. A., Anderson, B. F., Groom, C. R., Haridas, M. & Baker, E. N. (1997). *J. Mol. Biol.* **274**, 222–236.

Navaza, J. (1994). *Acta Cryst.* A**50**, 157–163.

Otwinowski, Z. & Minor, W. (1997). *Methods Enzymol.* **276**, 307–326.

Ramachandran, G. N. & Sasisekaran, V. (1968). *Adv. Protein Chem.* **23**, 283–438.

Rossmann, M. G. (1972). *The Molecular Replacement Method.* New York: Gordon & Breach.

Sharma, A. K., Kumar, S., Sharma, V., Nagpal, A., Singh, N., Tamboli, I., Mani, I., Raman, G. & Singh, T. P. (2001). *Proteins Struct. Funct. Genet.* **40**, 423–434.

Sharma, A. K., Paramasivam, M., Srinivasan, A., Yadav, M. P. & Singh, T. P. (1999). *J. Mol. Biol.* **289**, 303–317.

Sharma, A. K., Rajshankar, K., Yadav, M. P. & Singh, T. P. (1999). *Acta Cryst.* D**55**, 1152–1157.

Sharma, A. K. & Singh, T. P. (1999*a*). *Acta Cryst.* D**55**, 1792–1798.

Sharma, A. K. & Singh, T. P. (1999*b*). *Acta Cryst.* D**55**, 1799–1804.

Wilson, A. J. C. (1942). *Nature (London)*, **150**, 152.

Wootton, I. D. P. (1964). *Microdialysis in Medical Biochemistry*, 4th ed., p. 124. London: Churchill.